1-1-2016

Acetylated bacterial cellulose coated with urinary bladder matrix as a substrate for retinal pigment epithelium

Sara Goncalves
Universidade do Minho

Ines P. Rodrigues
Universidade de Coimbra

J Padrão
University of Minho

J P. Silva
University of Minho

Vitor Sencadas
University of Wollongong, victors@uow.edu.au

See next page for additional authors

Acetylated bacterial cellulose coated with urinary bladder matrix as a substrate for retinal pigment epithelium

Abstract

This work evaluated the effect of acetylated bacterial cellulose (ABC) substrates coated with urinary bladder matrix (UBM) on the behavior of retinal pigment epithelium (RPE), as assessed by cell adhesion, proliferation and development of cell polarity exhibiting transepithelial resistance and polygonal shaped-cells with microvilli. Acetylation of bacterial cellulose (BC) generated a moderate hydrophobic surface (around 65°) while the adsorption of UBM onto these acetylated substrates did not affect significantly the surface hydrophobicity. The ABS substrates coated with UBM enabled the development of a cell phenotype closer to that of native RPE cells. These cells were able to express proteins essential for their cytoskeletal organization and metabolic function (ZO-1 and RPE65), while showing a polygonal shaped morphology with microvilli and a monolayer configuration. The coated ABC substrates were also characterized, exhibiting low swelling effect (between 1.5-2.0 swelling/mm3), high mechanical strength (2048MPa) and non-pyrogenicity (2.12EU/L). Therefore, the ABC substrates coated with UBM exhibit interesting features as potential cell carriers in RPE transplantation that ought to be further explored.

Keywords

pigment, retinal, substrate, matrix, bladder, urinary, coated, epithelium, acetylated, cellulose, bacterial

Publication Details

Goncalves, S., Rodrigues, I. Patricio., Padrão, J., Silva, J. Pedro., Sencadas, V., Lanceros-Méndez, S., Girao, H., Gama, F. M., Dourado, F. & Rodrigues, L. R. (2016). Acetylated bacterial cellulose coated with urinary bladder matrix as a substrate for retinal pigment epithelium. Colloids and Surfaces B: Biointerfaces, 139 1-9.

Authors

Sara Goncalves, Ines P. Rodrigues, J Padrão, J P. Silva, Vitor Sencadas, Senentxu Lanceros-Méndez, Henrique Girao, F M. Gama, F Dourado, and L R. Rodrigues

Acetylated Bacterial Cellulose Coated with Urinary Bladder Matrix as a Substrate for Retinal Pigment Epithelium

Sara Gonçalves [a], Inês Patrício Rodrigues [b,†], Jorge Padrão [a], João Pedro Silva [a], Vitor Sencadas [c,‡], Senentxu Lanceros-Mendez [c], Henrique Girão [b], Francisco M. Gama [a], Fernando Dourado [a], Lígia R. Rodrigues [a,]*

[a] Centre of Biological Engineering, University of Minho, Campus de Gualtar, 4710-057, Braga, Portugal

[b] Centre of Ophthalmology and Vision Sciences, IBILI-Faculty of Medicine, University of Coimbra, 3000-354, Coimbra, Portugal

[c] Center/Department of Physics, University of Minho, Campus de Gualtar, 4710-057, Braga, Portugal

* Corresponding author email address: lrmr@deb.uminho.pt

† Current address: Nuffield Laboratory of Ophthalmology, Department of Clinical Neurosciences, University of Oxford, Oxford OX3 9DU, England.

‡ Current address: School of Mechanical, Materials and Mechatronics Engineering, University of Wollongong, NSW 2522, Australia.

Paper Statistics: Words: 5726 (excluding references) / Tables: 1 / Figures: 6

ABSTRACT

This work aimed to evaluate the feasibility of acetylated bacterial cellulose (ABC) substrates coated with urinary bladder matrix (UBM) for the transplantation of Retinal Pigment Epithelium (RPE) in retinal degenerative diseases that affect millions worldwide. Acetylation of bacterial cellulose (BC) generated a moderate hydrophobic surface (around 65 º). Adsorption of UBM onto ABC slightly decreased the water contact angle (50 º) and enabled the development of a cell phenotype closer to that of native RPE in ABC substrates. In particular, these cells were able to express proteins essential for RPE cytoskeletal organization and metabolic function (ZO-1 and RPE65), while showing a polygonal shaped morphology with microvilli and a monolayer configuration. The substrates were also characterized, exhibiting low swelling effect (between 1.5-2.0 swelling mm^{-3}), mechanical strength (2048 MPa) and non-pyrogenicity (2.12 EU L^{-1}). Therefore, the ABC substrates coated with UBM showed a great potential to be applied as cell carriers in RPE transplantation.

Keywords: Acetylated bacterial cellulose; urinary bladder matrix; retinal degenerative diseases; retinal pigment epithelium.

1. Introduction

The RPE is a highly polarized monolayer of polygonal-shaped and pigmented epithelial cells with apical microvilli and basolateral infoldings [1]. This monolayer is maintained and stabilized by the cytoskeleton of individual cells and their interactions at the basolateral junctional complexes [2-4]. These junctional complexes or tight junctions are composed of zonular occludens-1 (ZO-1), occludin, claudins 1, 2, 5, 12 and AL [1]. The retinal pigment epithelium (RPE) performs several complex functions essential for visual function, namely light energy absorption, photoreceptor outer segments phagocytosis, outer blood-retina barrier, secretion of immunosuppressive and growth factors [1,5]. As outer blood-retina barrier, the RPE prevents the transport of molecules larger than 300 kDa via intracellular mediation [6]. To be able to perform its complex functions, RPE cells have unique morphological and functional polarity properties, with an expression and polarized distribution of receptors, transporters, channels and enzymes (many of these are markers of differentiated RPE) [5].

With age, the RPE may be affected, compromising retinal integrity and leading ultimately to retinal degenerative diseases such as age-related macular degeneration (AMD), which is the most common cause of blindness worldwide [7]. A promising therapeutic approach for AMD is the replacement of diseased RPE by healthy stem cell-derived RPE-like cells, transplanted as an integer epithelial sheet on a carrier substrate [8,9]. An optimal cell scaffold for RPE transplantation should simulate the RPE natural microenvironment; allow nutrient flow or biodegrade rapidly; maintain the RPE phenotype; exhibit favorable surgical properties and biocompatibility [9]. Recent studies for the development of BM prosthetic substrates include: polyethylene terephthalate and poly(L-lactide-co-ε-caprolactone); parylene, already patented for stem cell therapy to treat diseased or damaged ocular tissue; montmorillonite clay-based

polyurethane nanocomposite; copolymers of methyl methacrylate and poly(ethylene glycol) methacrylate; and gelatin-biofunctionalized polyimide membranes [10-14].

In our previous work, the feasibility of bacterial cellulose (BC) as a novel substrate for RPE culture was assessed [15]. Thin and heat-dried BC substrates were surface-modified via acetylation and polysaccharide adsorption, using chitosan and carboxymethyl cellulose. The ability of the modified BC substrates to promote RPE cell adhesion and proliferation *in vitro* was assessed. Briefly, acetylation of BC decreased its swelling and the amount of endotoxins. Surface modification of BC greatly enhanced the adhesion and proliferation of RPE cells. Acetylated BC (ABC) showed the highest elastic modulus. Although similar proliferation rates were observed among the modified substrates, ABC showed a higher initial cell adhesion. This difference could be mainly due to the moderately hydrophobic surface obtained after acetylation. Indeed, optimal cell adhesion has been described to occur in moderately hydrophobic surfaces (water contact angles in the 40-70 ° range) [16].

In the current work, the ability of acetylated bacterial cellulose (ABC) substrates to support the phenotype of RPE cells was further studied. To improve cell response, an extracellular matrix extracted from porcine urinary bladder was used, the so-called urinary bladder matrix (UBM). The ultimate purpose was to assess the potential of these substrates as cell carriers in RPE transplantation. Bacterial cellulose (BC) holds unique structural and mechanical properties, such as permeability to gas and fluid exchange, biocompatibility and non-toxicity [8,12,17,18]. In fact, BC has shown to be an interesting and versatile biomaterial, particularly in tissue-engineered applications (tissue scaffolds and drug delivery systems) for the regeneration of damaged or diseased tissues and organs [19-21]. Also, UBM has been widely studied in several pre-clinical studies as a biologic scaffold for the reconstruction of damaged tissues [22-28].

Therefore, ABC substrates with and without UBM were first characterized according to their surface properties (hydrophobicity, free energy, topography, chemical composition), dimensional stability (swelling and handling stability), mechanical properties and endotoxins content. Cell viability and cytotoxicity assays were then performed to evaluate the ability of RPE cells to adhere and proliferate in the developed substrates. Finally, the expression of specific RPE markers and the development of cell polarity exhibiting transepithelial resistance and polygonal shaped-cells with microvilli, which are indicators of an adequate RPE cell morphology, were evaluated. The markers studied were the junctional ZO-1 protein and the retinal pigment epithelium-65 (RPE65), which is a RPE specific protein involved in the process of the visual cycle of retinal [1,4]. To the authors knowledge this is the first time such a specific study is conducted using BC as a substrate for RPE cells adhesion and proliferation.

2. Experimental

2.1. Reagents

Analytical grade acetic anhydride, acetic acid, toluene and perchloric acid were purchased from Merck (United States of America, USA), Fisher Chemical (USA), Fisher Chemical and Panreac (Spain), respectively. Rat-tail collagen type-I was purchased from BD Biosciences (USA). Cell culture reagents were purchased from Biochrom (Germany). The Pierce® BCA Protein Assay Kit, the Pierce® limulus amebocyte lysate (LAL) chromogenic endotoxin quantitation kit, the Invitrogen™ LIVE/DEAD Viability/Cytotoxicity kit for mammalian cells, Whatman™ polyethersulfone (PES) filters and Sigma Mowiol® mounting solution were purchased from Thermo Fisher (USA). The [3-(4,5-dimethylthiazol-2-yl)-5-(3-carboxymethoxyphenyl)-2-(4-

sulfophenyl)-2H-tetrazolium (MTS) was purchased from Promega (USA). The primary antibodies rabbit polyclonal anti-ZO1 immunoglobulin type G (IgG, 61-7300) and mouse monoclonal anti-RPE65 IgG (Ab13826) were purchased from Life Technologies and Abcam, respectively. The secondary antibodies were purchased from Life Technologies, namely goat anti-rabbit IgG (Alexa Fluor® 488, A11034) and goat anti-mouse IgG (Alexa Fluor® 488, A11001). The phosphate buffer saline (PBS) solution was prepared with 137 mM NaCl, 2.7 mM KCl, 8 mM Na_2HPO_4, and 2 mM KH_2PO_4 (pH 7.4).

2.2. Acetylated bacterial cellulose (ABC) substrates preparation

BC was produced by static culture of *G. xylinus* (*ATCC ® 53582™*) as previously described [15,29,30]. Briefly, fermentation was performed in 1 L Erlenmeyer flask with 200 mL of Hestrin-Schramm medium for 1 month. The resulting BC sheet was washed at room temperature (RT) with abundant tap water to remove residual medium, and placed for 24 h in a 1.0 N NaOH solution to remove bacteria and pyrogens. Alkaline residues were removed by washing thoroughly with distilled water until the final pH of the supernatant became that of distilled water. Then, the washed BC sheets were sliced into thin pellicles, dried in an oven at 50 °C for 8 h and cut into the desired geometric shapes with an average thickness of 61.5 ± 4.8 μm (5 and 9 mm diameter circles for 96 and 48 well plates, respectively, and 4.5 mm per 20 mm rectangles). BC was oven-dried, since never-dried BC has a much higher water-holding capacity [31]. Hence, thinner substrates with decreased swelling effect could be obtained (which is highly desirable given the envisaged application). The acetylation reaction mixture was composed of 40 mL acetic acid, 50 mL toluene and 0.2 mL perchloric acid. Oven-dried BC samples were added in a ratio of 1 cm^2 of substrate surface area per 1 mL reaction mixture. A volume of 8 ml of acetic anhydride and 15 min reaction time were used to generate a moderate hydrophobic surface

(water contact angle: 64.8 ± 1.9 °). After being washed and sterilized in 100 % ethanol, ABC substrates were maintained in sterile distilled water until use. ABC surface was also coated with UBM, as further described below.

2.3. Urinary bladder matrix (UBM) preparation, characterization and coating

UBM extraction was performed according to the method reported by Freytes *et al*. [23] and consists in separating the basement membrane of the urothelial cells and subjacent *lamina propria* from porcine bladders (kindly provided by a local slaughterhouse). After being washed with PBS solution and sterile water, UBM sheets were lyophilized, triturated, and kept at -20 °C until use. UBM was enzymatically digested immediately before being applied onto the substrates at 37 °C in 0.01 N HCl solution (pH 3-4). Two digestion conditions were studied, namely 10 g L^{-1} UBM and 1 g L^{-1} pepsin (reported by Freytes *et al*. [23]) and 20 g L^{-1} UBM and 3 g L^{-1} pepsin. These conditions were studied for up to 48h of digestion to determine which conditions allowed obtaining higher protein content within the UBM's typical protein profile. The digested UBM solution was centrifuged (20 min, 9000 x g) to remove insolubilized particles and then sterilized (0.22 μm PES filters). The protein content of the digested UBM solution was analyzed by sodium dodecyl sulfate polyacrylamide gel electrophoresis (SDS-PAGE) and the bicinchoninic acid (BCA) quantitation method. UBM and collagen type-I were electrophoresed on 10 % polyacrylamide gels under reducing conditions (5 % 2-mercaptoethanol) and stained with Coomassie Blue for proper visualization. The BCA Protein Assay Kit was used in accordance with the manufacturer guidelines, using bovine serum albumin as standard. Pepsin inactivation occurred after increasing the pH to 7.4 with 90 μL 1 N NaOH and 1.01 mL 10X concentrated PBS added to 9 mL sterile UBM solution. UBM gelation and coating on the

substrates occurred at 37 °C for 18 h with 100 μL cm^{-2} sample surface area. An excess of UBM was used to coat the acetylated membrane in order to guarantee its surface saturation.

2.4. Substrate characterization

Fourier transform IR spectroscopy in attenuated total reflectance mode (ATR-FTIR) was performed at RT to assess the surface chemical composition through the identification of surface functional groups. The IR spectra generated using a Perkin-Elmer Spotlight 300 FTIR microscope with Spectrum 100 FTIR spectrometer (USA), corresponded to the average of 100 scans measured at a resolution of 4 cm^{-1}. The vibration transition frequencies of each spectrum were baseline corrected and the absorbance was normalized between 0 and 1. Static contact angle measurements were performed using the sessile drop technique to determine the surface free energy (SFE, γ) and hydrophobicity. The water contact angle is an indirect indication of the degree of hydrophobicity. For SFE estimation, the van Oss-Chaudhury-Good (vOCG) method was used. Further details on this methodology are reported in Gonçalves *et al*. [15]. Substrate thickness measurements were performed using a Mitutoyo digital micrometer (Nº 293-5, Japan). To assess substrate swelling, the ABC substrates were placed in PBS solution and weighed at different time points, before and after (which was performed after 12 weeks) UBM adsorption. Simultaneously to the gravimetric procedures, handling stability was also evaluated by manipulating the membranes with tweezers. Since the samples presented variable thicknesses (average 61.5 ± 4.8 μm), swelling data taken individually (twelve replicas) were normalized with their respective initial volume as shown in **Equation (1)**, where $Mass_{dry}$ is the initial mass in dry state, and $Mass_{wet}^{t}$ is the mass measured in wet state at each time point, t.

$$\text{Swelling/ Volume} = \frac{\text{Mass}^{t}_{wet} - \text{Mass}_{dry}}{\text{Mass}t_{dry} \times \text{Volume}} \qquad (1)$$

Stress-strain assays were performed in tensile mode using a Shimadzu Universal Testing Machine, AG-IS with a 50 N load cell (Shimadzu Scientific Instruments, USA) to evaluate the substrates' mechanical properties, at RT and with a strain rate of 0.5 $mm.min^{-1}$. The samples were immersed for approximately 5 min in distilled water immediately prior to the tensile tests. Maximum stress (σ_{max}) and strain-to-failure (ε_{break}) were determined and the elastic modulus (E) was calculated from the stress-strain data of five replicas per substrate in the linear zone of elasticity, between 0 and 1 % of strain. BC substrates were analyzed for the presence of endotoxin using the LAL kit according to the supplier instructions. Each sterile ABC substrates of approximately 0.88 mm^3, with and without UBM, were immersed in 40 mL pyrogen-free water. The reaction was stopped with 25 % acetic acid and the absorbance measured at 405 nm.

2.5. Cell culture

Human RPE cells (hTERT-RPE1, ATCC CRL-4000) immortalized by the transfection with human telomerase gene (hTERT) have been reported to exhibit a normal RPE phenotype [32]. Cells were grown in Dulbecco's MEM/Ham's F12 (1:1 mixture) culture media supplemented with 10 % v/v fetal bovine serum (FBS), 100 U mL^{-1} penicillin and 100 µg mL^{-1} streptomycin (DMEM/F12 complete medium) at 37 °C in a humidified atmosphere of 95 % air and 5 % CO_2. At confluence, hTERT-RPE cells were harvested with 0.05 % (w/v) trypsin-EDTA and were sub-cultured in the same medium. PBS was used for all washing steps. For the viability assays, the media used consisted of DMEM (without phenol red) supplemented with 100 U mL^{-1} penicillin and 100 µg mL^{-1} streptomycin. Cells were seeded on the substrates and control surfaces at a density of 40,000 cells cm^{-2}.

2.6. Cell viability and proliferation

Cell viability was assessed at three time points (3, 7 and 14 days) to evaluate cell proliferation, using the [3-(4,5-dimethylthiazol-2-yl)-5-(3-carboxymethoxyphenyl)-2-(4-sulfophenyl)-2H-tetrazolium (MTS) assay and the LIVE/DEAD Viability/Cytotoxicity kit for mammalian cells. The MTS assay measures the metabolic activity of viable cells via its dehydrogenase activity. Briefly, cells were washed and incubated for 2 h with 20 µL MTS solution reagent in 100 µL EM; and afterwards the absorbance was recorded at 490 nm in a microplate reader. The LIVE/DEAD kit provides a two-color fluorescence cell viability assay, based on the simultaneous determination of live (green) and dead (red) cells with two probes, Calcein AM and Ethidium Homodimer (EthD-1), that measure intracellular esterase activity and loss of plasma membrane integrity, respectively. Cell cultures were incubated for 30 min at 37 °C in 10 % LIVE/DEAD working solution (2 µM EthD-1 and 4 µM Calcein AM in PBS pH 7.4) in EM. The substrates were then observed under a Leica DMIRE2 fluorescence microscope with a DFC350FX camera (Germany). Tissue culture polystyrene (TCP) surface was used as positive control to evaluate cell response in ABC substrates with and without UBM, in three independent experiments.

2.7. Immunofluorescence

RPE cell monolayers grown on glass coverslips (positive control surface) and on ABC+UBM substrates were fixed in ice-cold methanol for 5 min at RT and then carefully washed 3 times in PBS, 5 min each. Cells were incubated in permeabilization and blocking (perm/block) solution (0.05 % saponin and 0.5 % BSA in PBS), for 45 min at RT in a humidified chamber. This perm/block solution was also used to wash the cells between the following steps. Cells were

incubated with rabbit polyclonal antibody anti-ZO1 IgG (1:100, Life Technologies, 61-7300) or mouse monoclonal antibody anti-RPE65 IgG (1:200, Abcam, Ab13826) in perm/block solution for 2 h. Samples with no primary antibody's incubation were used as negative control. Afterwards, cells were incubated with the appropriate fluorophore-conjugated secondary antibodies (1:2000 in perm/block solution) for 30 min, namely goat anti-mouse IgG for RPE65 and goat anti-rabbit IgG for ZO-1. Finally, nuclei counterstaining using DAPI was performed and samples embedded with Mowiol® mounting solution under a coverslip and examined with a LSM 710 Meta confocal laser-scanning microscope (Zeiss, Germany).

2.8. Transepithelial resistance (TER)

TER assays can be used to measure the epithelial barrier function through the quantification of the cell-polarized level. The TER assays were performed with cells cultured in Transwell® insert chambers and using an epithelial voltohmmeter (EVOM) according to the protocol described by Sonoda *et al*. [4]. Briefly, measurements with the electrodes of the EVOM were made at RT after 20 min of stabilization, to minimize the TER fluctuation with temperature. The values of TER were measured with cells in a confluent monolayer configuration. Near the full confluent state, the FBS was reduced to 1 % to prevent cell overgrowth and to maintain a consistent cell monolayer in culture. Net TERs were calculated by subtracting from the experimental values the corresponding value of unseeded fibronectin-coated filters or filters with UBM-coated ABC substrates. Final resistance-area products (Ω cm^2) were obtained by the multiplication with the effective growth area.

2.9. Scanning electron microscopy (SEM)

For the cell morphology analysis, substrates subjected to cell culture for 14 days were fixed with 2.5 % glutaraldehyde in PBS pH 7.4 for 1 h, washed with distilled water, dehydrated through several ethanol changes (namely in 55, 70, 80, 90, 95 and 100 %, 30 min each), sputtered with gold and transferred to the microscopic carrier. For surface observation, the substrates were only dehydrated, sputter coated with gold and transferred to the microscopic carrier for observation under a Leica Cambridge S360 scanning electron microscope (Germany) with electron beam energy of 15 KV.

2.10. Statistics

All results are presented as the mean ± standard error mean of several independent experiments. Statistical analysis of variance (ANOVA) and the Tukey multiple comparisons post-test were used to compare results between different substrate conditions. Statistical differences were assigned to groups with a p-value lower than 0.05.

3. Results and discussion

3.1. UBM characterization

The UBM digestion conditions previously reported by Freytes *et al*. [23] were 10 g UBM and 1 g Pepsin per litter of 0.01 N HCl, for 48 h at 25 °C. In this work, shorter digestion periods at 37 °C, and higher initial amounts of UBM (20 g L^{-1}) and pepsin (3 g L^{-1}) were also evaluated. The protein content of the digested UBM was analyzed using protein electrophoresis (**Fig. 1. A - I**), to observe the protein profile in the soluble fraction and the amount of protein lost in the pellet. The protein content of the UBM soluble fraction was also quantified using the BCA method for

two digestion conditions (20 g L^{-1} UBM + 3 g L^{-1} pepsin and 10 g L^{-1} UBM + 1 g L^{-1} pepsin) and at several digestion time points up to 48 h (**Fig. 1**. **J, K**). The results showed that using 10 g L^{-1} UBM and 1 g L^{-1} of pepsin and shorter digestion times, the amount of protein of higher molecular masses increases (**Fig. 1. C - F**).

Well-defined bands characteristic of the collagen type-1 can be visualized in samples C, G and I (as digested with 20 g L^{-1} UBM and 1 g L^{-1} pepsin), which is in accordance with the ones reported in the literature [23,28]. After 6 h of digestion using 20 g L^{-1} UBM and 1 g L^{-1} of pepsin (**Fig. 1. G**), yielded a soluble fraction with higher protein content. However, a significant amount of protein remained in the pellet fraction, following centrifugation (**Fig. 1. H**). The amount of pepsin was then increased (from 1 to 3 g L^{-1}) and digestion was let to occur for 12 h to allow solubilizing more protein. These observations were further corroborated with quantitative data (**Fig. 1. J, K**), where higher initial concentrations of UBM and pepsin (**Fig. 1. J**) led to higher levels of protein concentration after UBM digestion and centrifugation. Thus, 20 g L^{-1} UBM and 3 g L^{-1} pepsin for 12 h of digestion were used to prepare the UBM solution to further coat the ABC substrates, since higher protein concentration (5.5 ± 0.2 g L^{-1}) with the correct protein profile was obtained. Additionally, besides the protein bands related to collagen type-1, other bands of lower molecular weights were observed that have been reported as being related to other elements present in UBM such as glycosaminoglycans and the glycoprotein fibronectin [23]. This confirms that UBM was successfully extracted from the porcine urinary bladders. Moreover, the results indicate that only 20–30 % (w/w) of the initial undigested lyophilized UBM mass was obtained in the soluble protein mass (**Fig. 1. J**). Therefore, the remaining mass weighted initially of lyophilized UBM was not solubilized in the digestion process and it was mainly lost in the centrifuged pellet.

3.2. Substrate characterization

The substrates were characterized according to their surface chemical composition, dimensional stability, mechanical strength, surface topography, endotoxin content, surface wettability and free energy. The ABC surface composition, based on acetate related functional groups, was confirmed by ATR-FTIR spectroscopy (**Fig. 2. A**). The typical absorbance bands of ABC substrates correspond to the ester C=O stretch at 1750 cm^{-1}, the alkane –C–H bending at 1355 cm^{-1}, and the two peaks relative to the ester C–O stretch at 1210 and 1025 cm^{-1}[15,33,34]. After UBM coating, the substrates displayed additional absorbance bands related to the collagen type-1, namely the amide I and amide II bands at 1650 and 1560 cm^{-1}, respectively. Three weaker bands that represent amide III vibration modes centered at 1245 cm^{-1} are also characteristic of the collagen FTIR spectrum [35]. However, these were not easily detected in the spectrum, similarly to other reports of protein immobilization where the bulk phases IR adsorption is strong [36]. This is due to the several hundreds of nanometers sampling depth of ATR-FTIR, comparing to only several to tens of nanometers of protein-grafted layers' thickness. In this case, the C–O stretch at 1210 cm^{-1} from the acetylation layer may be masking the amide III vibration bands at 1245 cm^{-1}.

The surface free energy and hydrophobicity properties were evaluated as they may influence the protein and cellular adhesion. As the substrates may present some roughness, the ideal contact angles (which include the roughness factor), could not be reported. Instead, the apparent contact angles were measured (**Table 1**), since they were considered equally valid to assess surface hydrophobicity and free energy [37].

The moderate hydrophobic character of ABC was maintained after UBM coating, although ABC substrates exhibited a decrease in the water contact angles from 64.8 ± 1.9 to 49.6 ± 1.8 °. This decrease in surface hydrophilicity may be due to a decrease in surface hydroxyl groups after UBM coating. The dispersive (γ^{LW}) and polar (γ^{AB}) energy components were roughly maintained after UBM coating being the first (around 42 mN m^{-1}) 10-fold higher than the latter, leading to similar values of surface free energy ($\boldsymbol{\gamma}$) (from 46.9 to 44.8 mN m^{-1}). Also, the acid-base forces ($\boldsymbol{\gamma^{AB}}$) resulted mainly from negative/basic charges ($\boldsymbol{\gamma^{-}}$), which showed an increase from 13.4 to 31.9 mN m^{-1} after UBM coating.

The maintenance of the mechanical integrity (resistance to tear) and dimensional stability (neither swelling nor degradation) are relevant properties in RPE transplantation, since the transplant success depends on the correct positioning of ultrathin substrates with surgical instruments in the subretinal space [14,38]. ABC substrates with and without UBM showed no signs of degradation (20 weeks exposure in PBS), were easily manipulated with tweezers and presented reduced swelling effect under prolonged immersion in PBS. Some swelling was observed in ABC substrates (**Fig. 2. B**), characterized by a two-fold increase in ABCs initial dry mass; however, this swelling stabilized after 4 weeks. The presence of UBM did not affect the swelling behavior on the stabilized ABC substrates (after 12 weeks), maintaining its initial mass and water holding capacity with prolonged immersion in PBS. According to its mechanical properties (**Table 1** and **Fig. 2. C**), both samples showed similar stress-strain behavior, with stress increasing with strain increment until the sample collapse. The presence of UBM resulted in a 3-fold increase in the elastic modulus (E), which suggests that it strongly adheres to sample fibers [19,39]. A porous surface could be observed in **Fig. 3.** for both substrates.

The mechanical properties of ABC+UBM are comparable to the ones reported in a recent study, where nanofibrous membranes of poly(lactic-*co*-glycolic acid) (PLGA) and collagen type-I (the main component of UBM) were evaluated as potential BM substitutes [3]. The values obtained for the PLGA nanofibrous membrane were 1.5 ± 0.4 MPa, 28.8 ± 4.9 % and 131.9 ± 13.3 MPa for maximum tensile strength, tensile strain and elastic modulus, respectively. On the other hand, higher values were obtained from the collagen nanofibrous membrane, namely 10.8 ± 0.7 MPa, 70.0 ± 4.6 % and 217.9 ± 15.3 MPa for maximum tensile strength, tensile strain and elastic modulus, respectively. In this work, the values obtained for the developed BC substrates are in the same range or even higher, thus suggesting its mechanical feasibility as a cell carrier substrate for the potential RPE transplantation therapy in retinal degenerative diseases. Also, the porous nature of these substrates is advantageous since a non-biodegradable substrate has to meet the passive diffusion requirements to be considered a viable BM substitute.

Since BC is a biomaterial produced by a Gram-negative bacterium, the presence of endotoxins in BC may constitute a problem. Endotoxins can activate RPE cells to secrete excessive amounts of inflammatory cytokines in the retina, thus promoting RPE degeneration [40]. The endotoxin limit is 500 EU L^{-1} for general medical devices and 60 EU L^{-1} for devices that contact cerebrospinal fluid [41]. The endotoxin quantification obtained by the LAL test (performed in accordance with the FDA guideline) indicated an extremely low presence of endotoxins in ABC substrates, specifically 0.11 ± 0.01 and 2.12 ± 0.04 EU L^{-1} before and after UBM coating, respectively. The substrates can therefore be classified as non-pyrogenic and should not induce complications *in vivo.* These results are in accordance with the literature, where the short and common purification/depyrogenation method of treating BC with an aqueous 1N NaOH solution, followed by rinsing with deionized sterile water, was found to be effective in

thin BC scaffolds [39]. UBM coating resulted in a 20-fold increase in the amount of endotoxins present in the ABC substrates. This may be due to microbial contamination of the porcine urinary bladders that led to the presence of endotoxins in the UBM solution. Similar endotoxin results have been reported for BC scaffolds produced by *G. xylinus* ATCC® 700198™ for tissue-engineered urinary conduits [39].

3.3. RPE cell viability and proliferation

Cell viability after 3, 7 and 14 days of cell culture on ABC substrates was assessed using metabolic activity (MTS) assays (**Fig. 4.**) and LIVE/DEAD fluorescence microscopy (**Fig. 5.**) of viable (green staining) and compromised (red staining of nucleus) cells. Regarding the metabolic activity after 3 days in culture, a difference in the number of adhered and metabolically active cells was observed between the ABC surfaces (with and without UBM) and the TCP positive control. Cells cultured on the ABC+UBM substrate and TCP surface showed the same metabolic activity after 3 days. Lower metabolic activity after 3 days was obtained for the ABC substrates without UBM coating as compared to TCP.

After 7 and 14 days, the cells were able to further proliferate and presented similar viability profiles as seen for the 3 days. Cells cultured in the TCP surface, achieved a 100 % confluent monolayer configuration after 7 days. The LIVE/DEAD fluorescence micrographs were coherent with the metabolic activity results, confirming the positive effect of UBM in cell viability leading to a profile similar to TCP. Additionally, while a confluent monolayer was obtained in TCP after 7 days and in ABC after 14 days, in the ABC+UBM substrates it appears to be reached between 7 and 14 days. The moderate hydrophobic surface composed of amine groups from the UBM proteins and acetate groups from the ABC substrates further improved the cell response to

a behavior similar to the one observed in the TCP positive control surface. Tezcaner *et al.* [42] reported that RPE cells preferred smooth rather than rough surfaces and that protein adsorption could modify the surface roughness by smoothing its irregularities. This might have contributed to the UBM positive effect on the cell response. Moreover, a similar RPE cell growth to the one obtained in the ABC with UBM substrates was reported with ultrathin collagen type-1 substrates and montmorillonite clay based polyurethane nanocomposite substrates [12,38].

3.4. RPE cell morphology

To evaluate the morphology of the RPE cell monolayers grown on the developed substrates, several cell parameters may be assessed, namely the expression of RPE proteins such as ZO-1 and RPE65, the observation of a polygonal shaped cells with apical microvilli in a monolayer configuration and the development of TER [1,3,4]. The RPE characteristic phenotype can be ascertained by the expression of RPE specific proteins. Immunofluorescence (IF) allows the observation of specific biomolecules and its cellular distribution. Two proteins were studied: the tight junction protein ZO-1 and the chaperone RPE-specific protein 65 kDa (RPE65), which is involved in the visual cycle of retinal. These are two of the most common RPE markers used to evaluate the development of differentiated properties of RPE cells in *in vitro* culture studies [38,43-45]. In IF assays, HTERT-RPE cells grown to confluence on glass and ABC with UBM (**Fig. 6.**), were able to express the structural protein ZO-1 and the metabolism protein RPE65, in the intracellular side of plasma membrane and cytoplasm, respectively.

Confluent cells grown on ABC substrates without UBM were also evaluated; however, these typical RPE phenotypic features were not observed (no fluorescence signal was detected, *data not shown*). These results suggest that although the cells were able to adhere and proliferate on

the ABC substrates, they were not able to develop the morphological features typical of RPE cells. Also, this confirms the positive effect of the UBM coating, and its important role in the development of a correct RPE phenotype. Moreover, although ZO-1 was clearly expressed in glass and ABC+UBM substrates (**Fig. 6. A, B**), the cells cultured in ABC+UBM still seem to be in the process of full differentiation as there was some ZO-1 in the cell cytoplasm. Also, the RPE65 protein was detected in the cytoplasm of both cultures (**Fig. 6. C, D**), which was expressed in small amounts when compared to ARPE-19 cells and primary cells [3,38]. Therefore, the hTERT-RPE1 cells may need longer periods in a confluent state to further organize their structure and proteins, or simply lower amounts of this protein are expressed in this cell line. To further observe the morphology of hTERT-RPE cells cultured in the ABC substrates coated with UBM, SEM pictures were taken (**Fig. 6. E, F, G**). This technique provided support that the cells were able to polarize in these substrates with the development of microvilli and the observation of a monolayer configuration with polygonal epithelial cell shape (white hexagon). Also, increasing number of microvilli (white arrows) was observed with prolonged culture time (from 10 to 20 days seen between **F** and **G**, **Fig. 6.**). The achievement of a cell monolayer between 7 and 14 days, as expected by the viability and proliferation results (**Fig. 4.** and **Fig. 5.**), was confirmed in the micrographs taken after 10 days of cell culture (**Fig. 6. E, F**). For the development of abundant sheet-like microvilli, human primary cells may be required as reported by Warnke *et al.* [3]. Nonetheless, the development of microvilli confirmed the ability of RPE cells to form a cell monolayer in a polarized state when cultured in ABC substrates coated with UBM. To further assess the polarized state of RPE cell monolayers grown in ABC substrates coated with UBM, transepithelial resistance quantification assays were performed. Although only human fetal or primary RPE cells have been described to develop

highly polarized RPE *in vitro*, studies on polarized RPE include the use of immortalized human RPE cell lines, such as the ARPE19 and D407 [4]. For sub-confluent or unpolarized RPE cells, no resistance to the passage of current was detected. Hence, in accordance with the previous morphological studies (IF and SEM), TER was detected in cells cultured in the ABC substrates coated with UBM. The average TER of cells in a confluent state maintained for 3 weeks in Transwell® inserts with fibronectin and in ABC+UBM substrates was 12.0 ± 0.7 and 10.2 ± Ω cm^2, with a maximum value of 17 and 13 Ω cm^2, respectively. To our knowledge, the TER values of hTERT-RPE cells have not been reported so far [32,46]. The TER herein presented for hTERT-RPE cells comprises low values (below 17 Ω cm^2), similarly to other immortalized cell lines (ARPE19 and D407) that were described to develop monolayers with TER values below 50 Ω cm^2[4,45,46]. Nonetheless, the even lower TER value obtained for hTERT-RPE cell is also supported by the reported down-regulation of proteins attributed to cell polarization in this cell line [47]. Additionally, several *in vitro* changes have been described in immortalized RPE cells, such as decreased apical microvilli and basal infoldings, low expression or absence of RPE-specific markers, among others [2]. These changes are most likely due to the lack of direct interaction and signaling from photoreceptors to the RPE apical surface. In fact, primary cultures are known to better retain the RPE native tissue physiology and morphological characteristics [2]. Therefore, these cultures should be explored in the future studies (such as phagocytosis assays for cell function analysis) to further assess the substrates potential for RPE transplantation. Nevertheless, the polarized RPE cell monolayers formed on the ABC substrates coated with UBM, using an immortalized cell line, reinforce the high potential of this biomaterial as a cell carrier for RPE transplantation.

4. Conclusion

The presence of UBM was found to be essential for the development of a typical RPE phenotype in the ABC substrates, namely a monolayer configuration, polygonal shaped cells with microvilli and the expression of cytoskeletal (ZO-1) and metabolic (RPE65) proteins. Additionally, these substrates showed some interesting features for the envisaged application, such as low swelling, no signs of degradation, easy manipulation, residual presence of endotoxins and mechanical strength. Further studies, such as *in vivo* biocompatibility assays and RPE cell function evaluation when cultured in these substrates, are required to confirm its feasibility for RPE transplantation.

Acknowledgments

The authors would also like to acknowledge José Ramalho for kindly supplying the RPE65 primary antibody. The authors acknowledge the Portuguese Foundation for Science and Technology (FCT, Portugal) for the financial support provided through the doctoral and pos-doctoral grants SFRH/BD/63578/2009, SFRH/BD/64901/2009, SFRH/BPD/64958/2009 and SFRH/BPD/63148/2009 for Sara Gonçalves, Jorge Padrão, João Pedro Silva, and Vitor Sencadas, respectively. The authors also acknowledge the projects PEst-OE/EQB/LA0004/2013, PEst-OE/EQB/LA0023/2013, PEST-C/FIS/UI607/2014, PTDC/BBB-BQB/2450/2012 and PTDC/SAU-ORG/118694/2010, co-funded by QREN, FEDER. Finally, the authors thank the FCT strategic project UID/BIO/04469/2013 unit, the project RECI/BBB-EBI/0179/2012 (FCOMP-01-0124-FEDER-027462) and the project “BioInd - Biotechnology and Bioengineering for improved Industrial and Agro-Food processes", REF. NORTE-07-0124-

FEDER-000028 co-funded by the Programa Operacional Regional do Norte (ON.2 – O Novo Norte), QREN, FEDER.

References

[1] O. Strauss, Physiol. Rev. 85 (2005) 845.

[2] V.L. Bonilha, Exp. Eye Res. 126 (2014) 38.

[3] P. Warnke, M. Alamein, S. Skabo, S. Stephens, R. Bourke, P. Heiner, Q Liu, Acta Biomater. 9 (2013) 9414.

[4] S. Sonoda, C. Spee, E. Barron, S.J. Ryan, R. Kannan, D.R. Hinton, Nat. Protoc. 4 (2009) 62.

[5] J. Adijanto, N.J. Philp, Exp. Eye Res. 126 (2014) 77.

[6] J.C. Booij, D.C. Baas, J. Beisekeeva, T.G.M.F. Gorgels, A.A.B. Bergen, Prog. Retin. Eye Res. 29 (2010) 1.

[7] L.S. Lim, P. Mitchell, J.M. Seddon, F.G. Holz, T.Y. Wong, Lancet 379 (2012) 1728.

[8] A.F. Carr, M.J.K. Smart, C.M. Ramsden, M.B. Powner, L. Cruz, P.J. Coffey, Trends Neurosci. 36 (2013) 385.

[9] S. Binder, B.V. Stanzel, I. Krebs, C. Glittenberg, Prog. Retin. Eye Res. 26 (2007) 516.

[10] Z. Liu, N. Yu, F.G. Holz, F. Yang, B.V. Stanzel, *Biomaterials* 35 (2014) 2837.

[11] M. Humayun, A. Ahuja, Y.C. Tai, D. Hinton, R. Grubbs, D. Clegg, US Patent 8,808,687; 2014.

[12] G.R. Silva, A. Silva-Cunha, L.C. Vieira, L.M. Silva, E. Ayres, R.L. Oréfice, S.L. Fialho, J.B. Saliba, F. Behar-Cohen, J. Mater. Sci. Mater. Med. 24 (2013) 1309.

[13] A.J. Treharne, H.A. Thomson, M.C. Grossel, A.J. Lotery, J. Biomed. Mater. Res. A 100 (2012) 2358.

[14] S. Julien, T. Peters, F. Ziemssen, B. Arango-Gonzalez, S. Beck, H. Thielecke, H. Büth, S. Vlierberghe, M. Sirova, P. Rossmann, B. Rihova, E. Schacht, P. Dubruel, E. Zrenner, U. Schraermeyer, Biomaterials 32 (2011) 3890.

[15] S. Gonçalves, J. Padrão, I.P. Rodrigues, J.P. Silva, V. Sencadas, S. Lanceros-Mendez, H. Girão, F. Dourado, L.R. Rodrigues, Biomacromolecules 16 (2015) 1341.

[16] Y. Arima, H. Iwata, Biomaterials 28 (2007) 3074.

[17] J.W. Miller, Am. J. Ophthalmol. 155 (2013) 1.

[18] L. Cruz, F.K. Chen, A. Ahmado, J. Greenwood, P. Coffey, Prog. Retin. Eye Res. 26 (2007) 598.

[19] L. Fu, J. Zhang, G. Yang, Carbohydr. Polym. 92 (2013) 1432.

[20] W. Lin, C. Lien, H. Yeh, C. Yu, S. Hsu, Carbohydr. Polym. 94 (2013) 603.

[21] W.K. Czaja, D.J. Young, M. Kawecki, R.M. Brown, Biomacromolecules 8 (2007) 1.

[22] S.F. Badylak, D.O. Freytes, T.W. Gilbert, Acta Biomater. 5 (2009) 1.

[23] D.O. Freytes, J. Martin, S.S. Velankar, A.S. Lee, S.F. Badylak, Biomaterials 29 (2008) 1630.

[24] R.L. Ringel, J.C. Kahane, P.J. Hillsamer, A.S. Lee, S.F. Badylak, J. Speech Lang. Hear. Res. 49 (2006) 194.

[25] A. Nieponice, T.W. Gilbert, S.F. Badylak, Ann. Thorac. Surg. 82 (2006) 2050.

[26] S.F. Badylak, D.A. Vorp, A.R. Spievack, A. Simmons-Byrd, J. Hanke, D.O. Freytes, A. Thapa, T.W. Gilbert, A. Nieponice, J. Surg. Res. 128 (2005) 87.

[27] J.D. Wood, A. Simmons-Byrd, A.R. Spievack, S.F. Badylak, J. Am. Vet. Med. Assoc. 226 (2005) 1095.

[28] D.O. Freytes, S.F. Badylak, T.J. Webster, L.A. Geddes, A.E. Rundell, Biomaterials 25 (2004) 2353.

[29] F. Andrade, R. Costa, L. Domingues, R. Soares, M. Gama, Acta Biomater. 6 (2010) 4034.

[30] R.A.N. Pertile, F.K. Andrade, C. Alves Jr., M. Gama, Carbohydr. Polym. 82 (2010) 692.

[31] D. Klemm, D. Schumann, U. Udhardt, S. Marsch, Prog. Polym. Sci. 26 (2001) 1561.

[32] L. Rambhatla, C. Chiu, R.D. Glickman, C. Rowe-Rendleman, Invest. Ophthalmol. Vis. Sci. 43 (2002) 1622.

[33] D. Kim, Y. Nishiyama, S. Kuga, Cellulose 9 (2002) 361.

[34] W. Hu, S. Chen, Q. Xu, H. Wang, Carbohydr. Polym. 83 (2011) 1575.

[35] B.C. Vidal, M.L. Mello, Micron 42 (2011) 283.

[36] Z. Ma, Z. Mao, C. Gao, Colloids Surf. B 60 (2007) 137.

[37] J. Kujawa, A. Rozicka, S. Cerneaux, W. Kujawski, Colloids Surf. A 443 (2014) 567.

[38] G. Thumann, A. Viethen, A. Gaebler, P. Walter, S. Kaempf, S. Johnen, A.K. Salz, Biomaterials 30 (2009) 287.

[39] A. Bodin, S. Concaro, M. Brittberg, P. Gatenholm, J. Tissue Eng. Regen. Med. 1 (2007) 406.

[40] K.W. Leung, C.J. Barnstable, J. Mol. Immunol. 46 (2009) 1374.

[41] Guideline on validation of the limulus amebocyte lysate test as an end-product endotoxin test for human and animal parenteral drugs, biological products and medical devices. U. S. Department of Health and Human Services, Public Health Service, Food and Drug Administration, Rockville, MD, 1987, p. 49-54.

[42] A. Tezcaner, K. Bugra, V. Hasirci, Biomaterials 24 (2003) 4573.

[43] B. Diniz, P. Thomas, B. Thomas, R. Ribeiro, Y. Hu, R. Brant, A. Ahuja, D. Zhu, L. Liu, M. Koss, M. Maia, G. Chader, D.R. Hinton, M.S. Humayun, IOVS 54 (2013) 5087.

[44] A. Vugler, A.J. Carr, J. Lawrence, L.L. Chen, K. Burrell, A. Wright, P. Lundh, M. Semo, A. Ahmado, C. Gias, L. Cruz, H. Moore, P. Andrews, J. Walsh, P. Coffey, Exp. Neurol. 214 (2008) 347.

[45] K.C. Dunn, A.E. Aotaki-Keen, F.R. Putkey, L.M. Hjelmeland, Exp. Eye Res. 62 (1996) 155.

[46] K. Vellonen, M. Malinen, E. Mannermaa, A. Subrizi, E. Toropainen, Y. Lou, H. Kidron, M. Yliperttula, A. Urtii, J. Control Release 190 (2014) 94.

[47] C.S. Alge, S.M. Hauck, S.G. Priglinger, A. Kampik, M. Ueffing, J. Proteome Res. 5 (2006) 862.

Figure Captions

Fig. 1. SDS-PAGE protein profiles (left side) of the following samples: molecular mass marker (A); rat-tail collagen type-1 (B); soluble fraction of urinary bladder matrix (UBM) after 6 h (C), 12 h (D), 24 h (E) and 48 h (F) of digestion using 10 g L^{-1} UBM and 1 g L^{-1} of pepsin; soluble fraction (G) and pellet (H) of UBM for 6 h of digestion using 20 g L^{-1} UBM and 1 g L^{-1} of pepsin; and soluble fraction of UBM after 12 h of digestion using 20 g L^{-1} UBM and 3 g L^{-1} of pepsin (I). Protein concentration (right side) of the UBM soluble fraction up to 48 h of digestion in two digestion conditions: (J) 20 g L^{-1} UBM + 3 g L^{-1} pepsin and (K) 10 g L^{-1} UBM + 1 g L^{-1} pepsin (results correspond to the mean ± standard error mean of three independent assays with three replicas each).

Fig. 2. (A) Infrared spectra, **(B)** swelling profile and **(C)** stress-strain measurements for acetylated bacterial cellulose (ABC) substrates, before and after (gray area) urinary bladder matrix (UBM) coating. The results correspond to the mean ± standard error mean of twelve replicas *per* condition for swelling assays and five replicas *per* condition for stress-strain assays.

Fig. 3. Surface scanning electron micrographs of acetylated bacterial cellulose (ABC) and urinary bladder matrix coated ABC (ABC+UBM) substrates.

Fig. 4. Metabolic activity determined after 3, 7 and 14 days of HTERT-RPE cells cultured on acetylated bacterial cellulose (ABC), ABC with urinary bladder matrix (ABC+UBM) substrates, and tissue culture polystyrene (TCP, control surface). Three independent assays were performed, each with six replicas *per* substrate condition. Equal letters above the bars indicate results not different statistically.

Fig. 5. Representative live/dead fluorescence micrographs of HTERT-RPE1 cells cultured for 3, 7, and 14 days on acetylated bacterial cellulose (ABC), ABC coated with urinary bladder matrix (ABC+UBM) and tissue culture polystyrene (TCP, control surface). The ABC+UBM micrographs presented higher substrate fluorescence interference.

Fig. 6. Immunofluorescence micrographs of ZO-1 (A and B) and RPE65 (C and D) green staining and nucleus blue staining in hTERT-RPE cells grown in glass (A and C) and in acetylated bacterial cellulose with urinary bladder matrix (ABC+UBM) substrates (B and D). Scanning electron micrographs of hTERT-RPE cell cultured in ABC+UBM substrates for 10 days (E and F) and 20 days (G). The cell monolayer configuration is observed in E, while the presence of microvilli is pointed out with white arrows (F and G) and the white hexagons highlight the polygonal shaped cells (F and G).

Figure 1

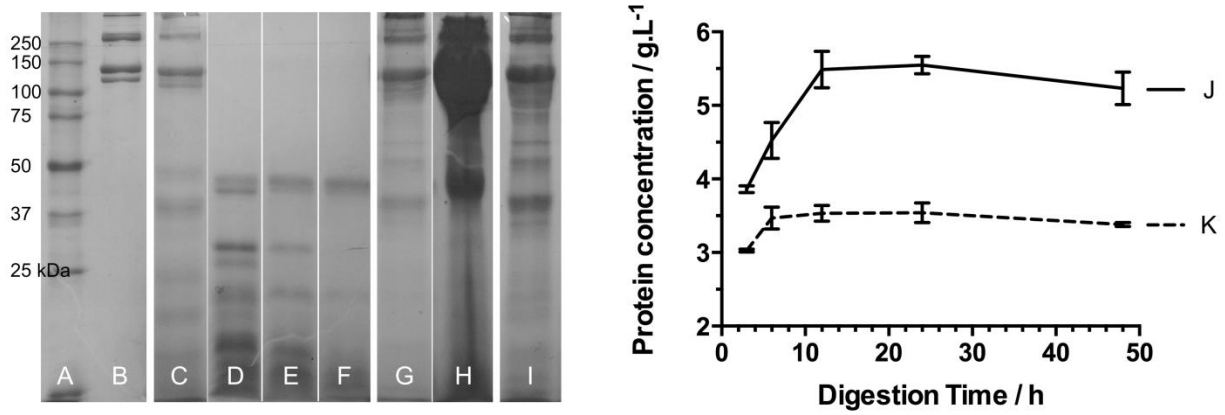
250
150
100
75
50
37
25 kDa
A
B
C
D
E
F
G
H
I
Protein concentration / g.L-1
Digestion Time / h
J
K

Figure 2

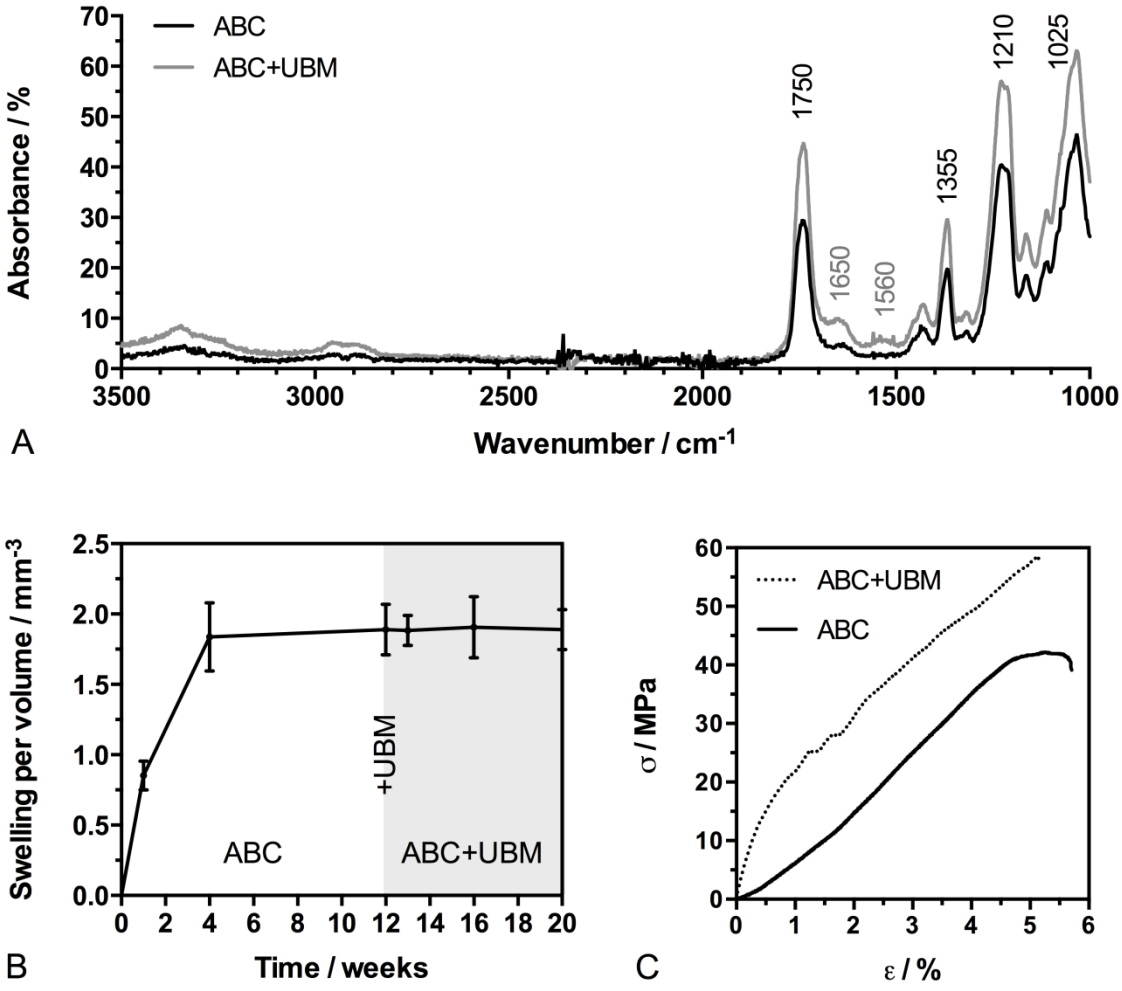
ABC
ABC+UBM
Absorbance / %
1750
1650
1560
1355
1210
1025
Wavenumber / cm-1
A
Swelling per volume / mm-3
+UBM
ABC
ABC+UBM
Time / weeks
B
σ / MPa
ε / %
C

Figure 3

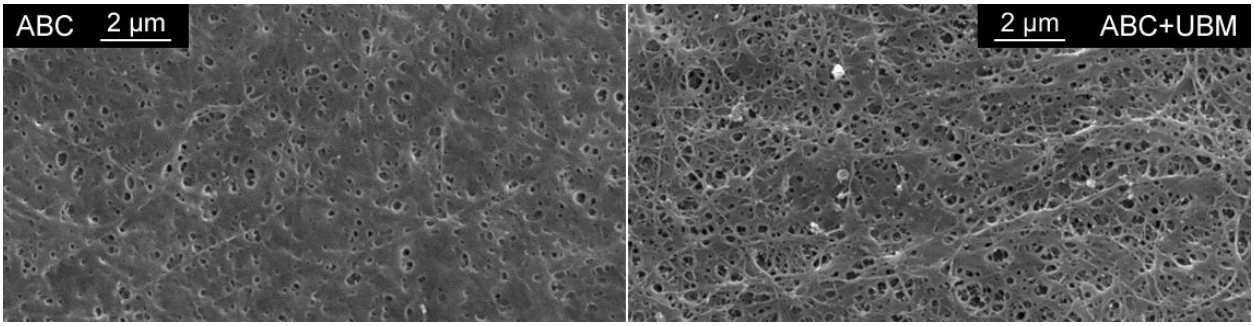

Figure 4

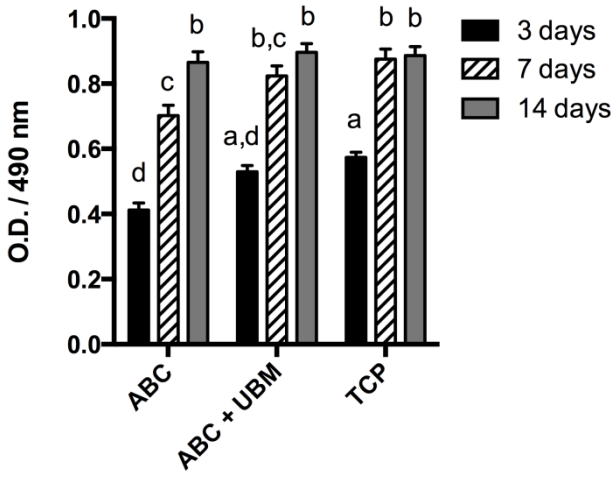
1.0
0.8
0.6
0.4
0.2
0.0
O.D. / 490 nm
d
c
b
a,d
b,c
b
a
b
b
ABC
ABC + UBM
TCP
3 days
7 days
14 days

Figure 5

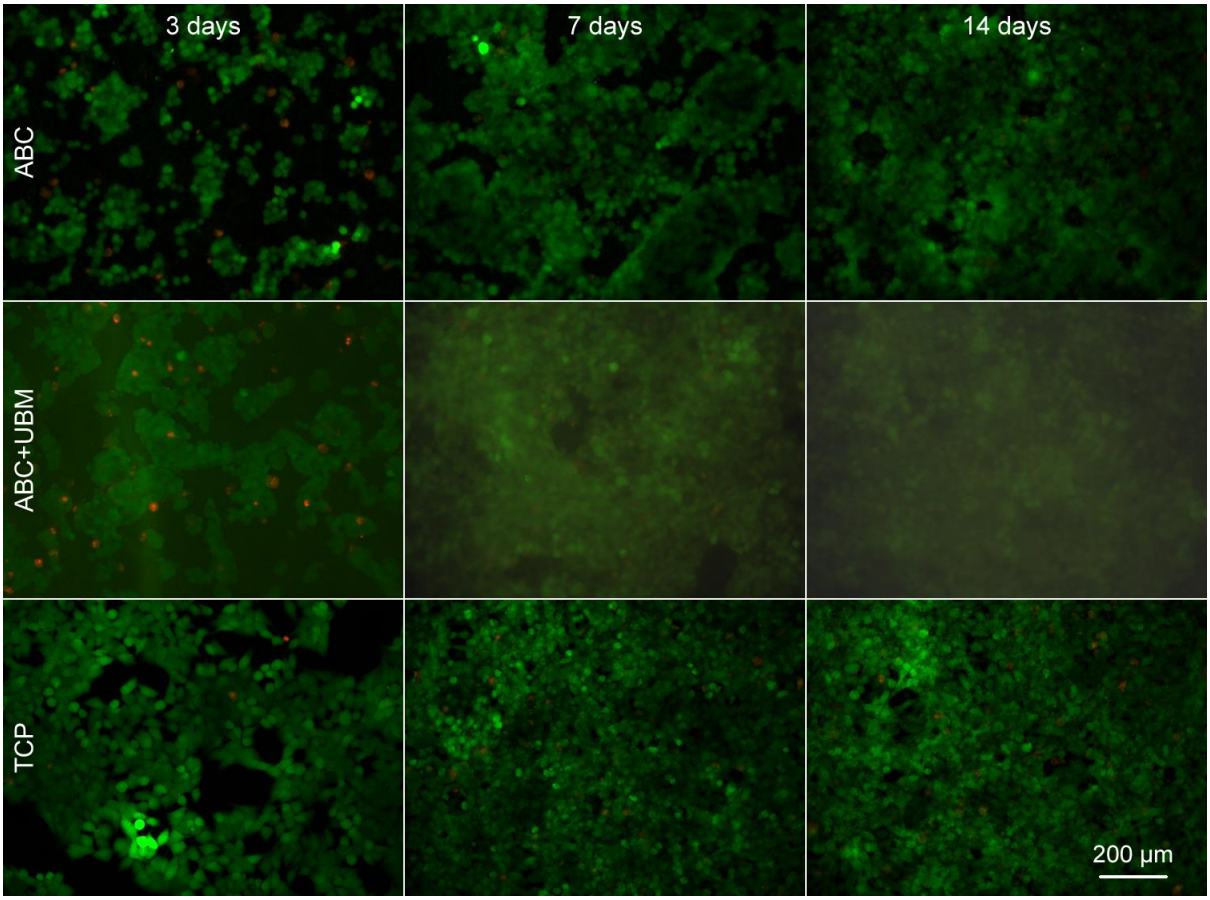

Figure 6

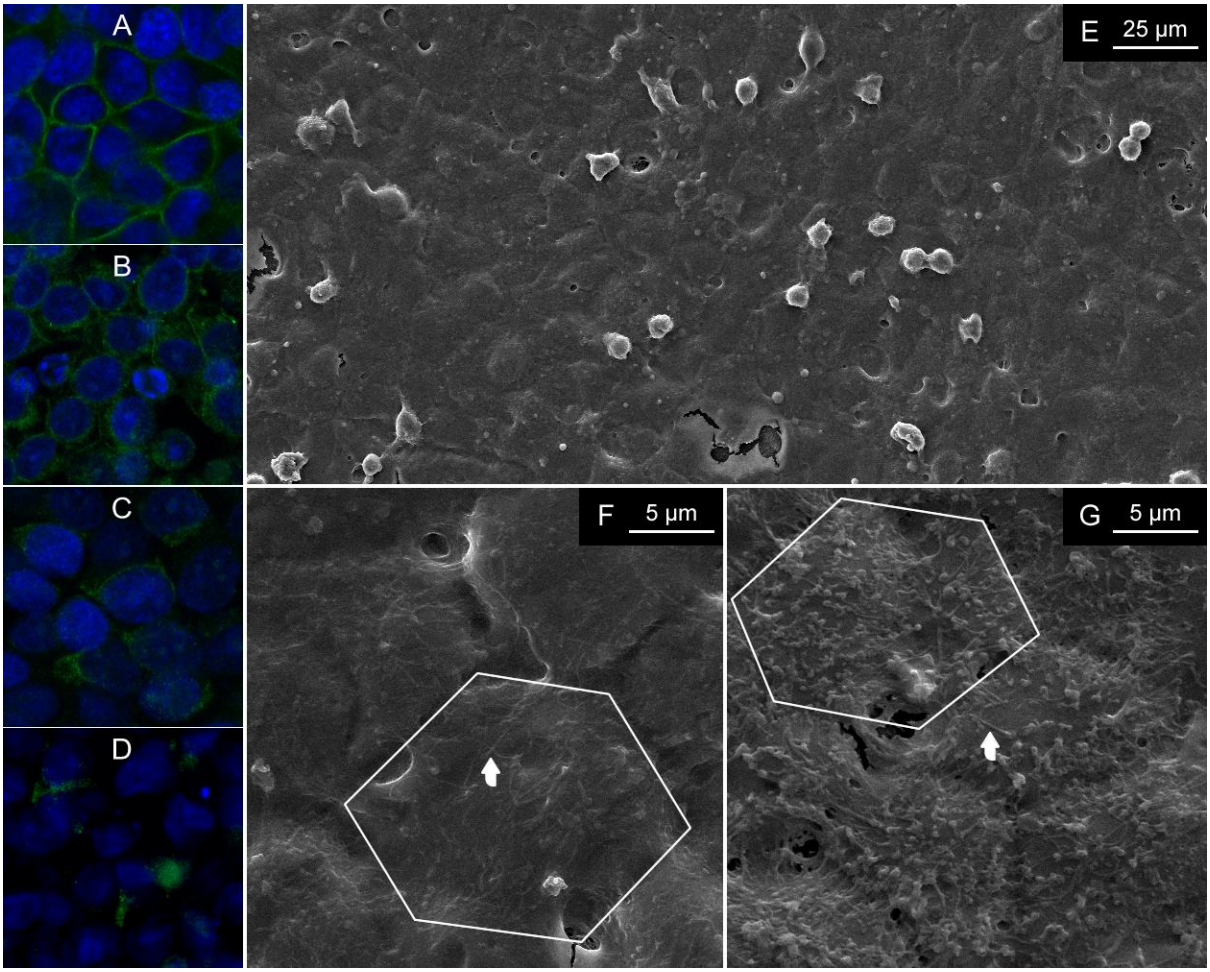

Table 1. Contact angles, estimated surface free energy components and mechanical properties of acetylated bacterial cellulose (ABC) uncoated and coated with urinary bladder matrix (UBM)

	ABC	**ABC+UBM**
Contact angles		
WCA / °	64.8 ± 1.9[e]	49.6 ± 1.8[f]
FCA / °	43.7 ± 1.4[g]	42.1 ± 1.6[g]
BCA / °	16.5 ± 0.6[h]	20.0 ± 0.7[i]
Surface free energy components		
γ^+ / mN m^{-1}	0.3	0.1
γ^- / mN m^{-1}	13.4	31.9
γ^{AB} / mN m^{-1}	4.3	3.0
γ^{LW} / mN m^{-1}	42.6	41.8
γ / mN m^{-1}	46.9	44.8
Mechanical Properties		
σ_{max}/ MPa	37.6 ± 4.4[a]	42.5 ± 4.3[a]
ε_{break} / %	4.8 ± 0.5[b]	5.1 ± 1.4[b]
E / MPa	677.5 ± 43.5[c]	2047.7 ± 192.3[d]

Abbreviations: σ_{max}, maximum stress; ε_{break}, elongation-at-break; E, elastic modulus; WCA, water contact angle; FCA, formamide contact angle; BCA, bromonaphthalene contact angle; γ^+, acidic parameter; γ^-, basic parameter; γ^{AB}, acid-base component; γ^{LW}, Lifshitz-van der Waals component; γ, total surface free energy. **Statistics**: five replicas *per* substrate in the mechanical assays and two contact angle measurements *per* replica with six replicas *per* substrate. Equal letters in superscript indicate that differences are not statistically significant.

Graphical abstract

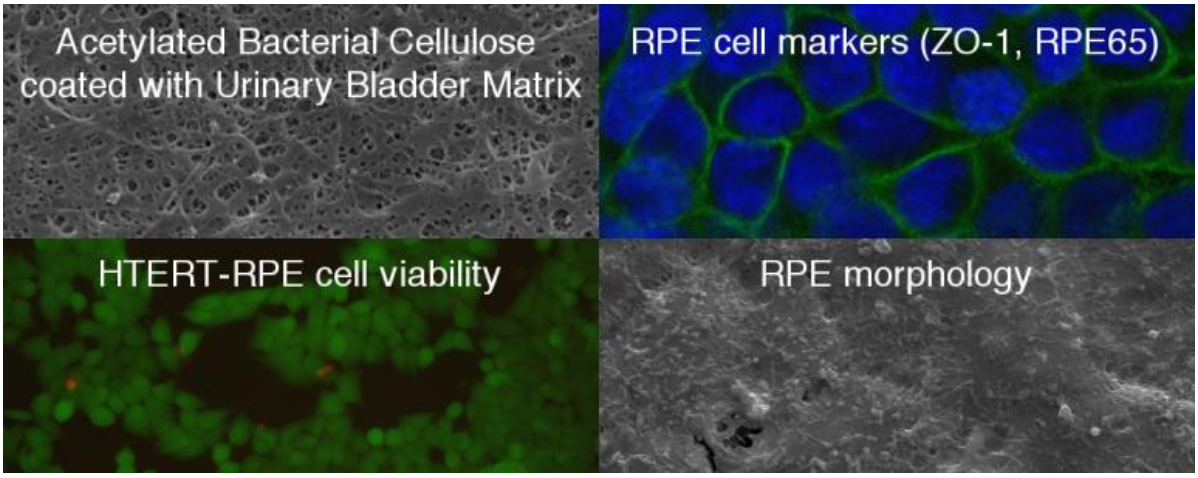

Highlights

1. Acetylated bacterial cellulose (ABC) substrates exhibit moderate hydrophobic surface
2. Urinary bladder matrix (UBM) has high protein content with an adequate profile to promote the adhesion a retinal pigment epithelium (RPE)
3. ABC substrates coated with UBM enable RPE transplantation
4. These substrates have reduced swelling effect, no signs of degradation, easy manipulation, mechanical strength and residual presence of endotoxins
5. RPE develops normal morphological features when adhered to these substrates